The Monte Carlo Method: Versatility Unbounded In A Dynamic Computing World
Chattanooga, Tennessee, April 17−21, 2005, on CD-ROM, American Nuclear Society, LaGrange Park, IL (2005)

FAST-NEUTRON SCATTERING ANGLE FROM INELASTIC SCATTERING

Hansem Joo
Bechtel Bettis, Inc.
P. O. Box 79
West Mifflin, PA 15122-0079
jooh@bettis.gov

ABSTRACT

An algorithm has been developed for accurately determining scattering angles of neutrons emerging from inelastic collisions of fast neutrons when a multi-group energy transfer matrix method is used. This new algorithm is designed to replace existing algorithm in the RCP01 Monte Carlo neutron transport code that uses an approximation for the direction of the exiting neutron. RCP01 solves neutron and photon transport problems in three dimensional geometry with the energy treated as a continuous variable. The new algorithm is based on a classical treatment of two-body collision kinematics with a stationary target nucleus and has no approximations, where the scattering angle in the laboratory coordinate system (LAB) is defined in terms of the center-of-mass coordinate system (CM) scattering angle and the LAB exit energy.

While multi-group methods for inelastic scattering are less exact than the discrete excitation energy level method used in other Monte Carlo codes, such as MCNP, they have computational advantages and are sufficiently accurate for a wide variety of fast and thermal reactor applications as shown by experience. In the multi-group method, an energy-group matrix is randomly sampled to determine the exit energy group, where each matrix element corresponds to the mean number of neutrons appearing in an exit energy group per inelastic scattering event in an incident energy group. The scattering angle from an anisotropic inelastic scattering event can be determined by using angular distribution functions specified either in the LAB or in the CM system.

Current ENDF inelastic scattering energy transfer functions for most nuclides are specified in terms of LAB energies, and only a few light nuclides are specified in terms of CM energies. Therefore, the multi-group matrices for fast inelastic scattering are usually defined in terms of LAB energies. However, the calculation of accurate LAB scattering angles requires corresponding CM exit energies. When the CM exit energy is unavailable, it may be approximated by using the LAB exit energy, as in RCP01. This approximation is accurate for heavy nuclides or for light nuclides in a confined realm of CM scattering angles. The approximation, however, is less accurate for other conditions. For example, when the CM scattering cosine is ±0.6 for graphite, the error in the LAB scattering angle could exceed 10%. The new algorithm eliminates the approximation and, therefore, the resulting errors.

Key Words: fast neutrons, inelastic scattering, scattering angle

1. INTRODUCTION

An algorithm has been developed which accurately determines scattering angles of neutrons emerging from inelastic collisions of fast neutrons with stationary target nuclei when the inelastic scattering is treated in a multi-group energy transfer matrix method in Monte Carlo neutron transport codes. The new algorithm is based on a classic two-body collision kinematics problem, requires no additional nuclear data or approximations pertaining to the inelastic scattering treatment, and is simple to implement.

In inelastic scattering, part of the kinetic energy of the incident neutron is expended in increasing the internal energy of one or both of the colliding particles. Changes in the internal energy of the colliding particles are treated in various ways in Monte Carlo neutron transport codes, and two common treatments are multi-group energy trans-

fer matrix methods [1, 2], and discrete compound-nucleus excitation-energy level methods [3, 4]. The new algorithm is designed to replace existing approximations used in the Monte Carlo code RCP01 [1], which uses a multi-group energy transfer matrix method for fast inelastic scattering. RCP01 solves neutron and photon transport problems in three dimensional geometry with the energy treated as a continuous variable.

In the RCP01 multi-group matrix method, a matrix element is equal to the mean number of neutrons appearing in an exit energy group per inelastic scattering event in an incident group. The matrix elements are used to randomly sample the exit energy group. Within an exit group, the exit energy is sampled uniformly. An exception is for within-group scattering, where the exit energy is constrained to be less than the incident energy. In the discrete excitation-energy level method, fast inelastic scattering is treated in a more detailed way. The excitation-energy levels of the compound nucleus are randomly sampled with probabilities proportional to the relative size of the inelastic cross section for that level. The exit energy and scattering angle are then determined by formulas appropriate to the scattering laws specified in ENDF [5] for that particular reaction. Either method usually ignores the motion of the target nucleus. While the multi-group matrix methods are somewhat inexact compared to the more rigorous discrete level methods, they have certain computational advantages (e.g., modest amount of nuclear data and faster sampling algorithm), and experience has shown that they are sufficiently accurate for a wide variety of fast and thermal reactor (in-core) applications.

The scattering angle of the outgoing neutron emerging from an inelastic scattering can be determined by using various angular distribution functions available in ENDF (e.g., functions specified in the center-of-mass coordinate system [to be called "the CM system"] for individual discrete excitation-energy levels), or by assuming an isotropic scattering in the CM system or even in the laboratory coordinate system [to be called "the LAB system"]. The angular distribution of inelastically scattered neutrons is somewhat simple over most of the energy range of interest in reactor theory. Up to around 10 MeV a large majority of these neutrons are emitted isotropically (i.e., not only independent of the azimuthal angle but also independent of the polar angle) − or nearly so − in the CM system for many nuclides of interest (e.g., ^{16}O, Zr isotopes, and ^{235}U). Above approximately 10 MeV, the angular distribution tends to become forward peaked and exhibits a scattering pattern similar to that found in elastic scattering at these energies (e.g., C and ^{56}Fe).

Multi-group energy transfer matrices for the inelastic scattering can be defined in terms of neutron incident and exit energies specified in either the LAB or the CM system. Currently in ENDF, the inelastic scattering energy transfer functions are specified primarily in terms of neutron incident and exit energies given in the LAB system, with the energy transfer functions of only a few light nuclides (atomic mass numbers not exceeding 4) described in terms of CM energies. Therefore, the inelastic multi-group energy transfer matrices used in RCP01 are defined in terms of neutron energies given in the LAB system. An accurate determination of the LAB scattering angle in RCP01 requires the CM exit energy corresponding to the LAB exit energy sampled from the RCP01 multi-group matrix method. Since a direct transformation of the LAB exit energy to the corresponding CM exit energy was unavailable, RCP01 has used an approximation: the CM exit energy ≈ the LAB exit energy. This approximation is accurate for very heavy targets or for limited conditions of certain neutron energy transfer or scattering angles (Figure 1). Otherwise, the approximation is judged inappropriate. For example, when the CM scattering angle cosine is ±0.6 for a particular condition, the error in the resulting LAB scattering angle could exceed 10% (Table I and Figure 3). Therefore, a new algorithm has been developed to replace the existing RCP01 approximation. The new algorithm is based on a classic two-body collision kinematics problem, where the LAB scattering angle is formulated directly in terms of the CM scattering angle and the LAB exit energy that are readily available from the RCP01 multi-group matrix method. No direct computation of or approximation regarding the CM exit energy is necessary.

Even though the principal subject of this paper is the LAB-to-CM exit energy transformation algorithm for fast inelastic scattering, the RCP01 multi-group energy transfer matrix method and exit neutron velocity vector determination methods are briefly described in Sections 2, 3 and 5. Section 4 presents a complete derivation and discussions of the new algorithm. Section 6 provides a summary.

2. MULTI-GROUP ENERGY TRANSFER MATRIX

The energy transfer matrix used in the RCP01 multi-group inelastic scattering method [1] is described here. For computational efficiency, the RCP01 code treats non-elastic (n,2n), (n,3n), and other (n,xn) reactions as a type

of inelastic scattering. A nuclear data library provides the inelastic scattering cross-section data combined with those of the (n,2n), (n,3n), and other (n,xn) reactions for each nuclide that undergoes an inelastic scattering. These combined cross-section data are tabulated over inelastic multi-groups 1 through N covering the fast energy range (usually above 5.53 keV), with group 1 being the highest energy group and group N being the lowest. It is assumed that no inelastic scattering occurs below 5.53 keV.

Elements of the inelastic scattering matrix for a nuclide are defined in terms of a probability distribution function in the following manner. Suppose $p^{n\to m}$ is the probability of neutron energy transfer from multigroup n to multi-group m during an inelastic scattering. The probability is determined in accordance with the definition of the "combined" inelastic cross section so that the probability can retain the weight gain due to (n,xn) reactions and thence its sum can exceed unity as discussed below. Then matrix elements a^{nm} can be obtained in a cumulative normalized form as follows:

$$a^{nm} = \sum_{g=n}^{m} p^{n\to g} \; for \; m \geq n \;\; and \;\; n = 1,2,..., N, \; and$$

$$a^{nm} = 0 \; for \; m < n \;\; and \;\; n = 2,..., N,$$

where the summation is performed over exit energy groups g=n through m. That is, no upscattering is allowed in the fast inelastic energy range, and thence the N-by-N inelastic scattering matrix is triangular. The matrices a^{nm} in RCP01 are defined in terms of neutron incident and exit energies specified in the LAB system.

The matrix elements give the mean number of neutrons produced in exit multi-groups n through m due to an inelastic scattering and neutron-producing (n,xn) events in the multi-group n. Element a^{nN} represents the total number of neutrons emerging from an inelastic scattering of a neutron having incident energy in multigroup n, which is equivalent to the ratio $[\sigma_{in} + 2\sigma_{n2n} + 3\sigma_{n3n} + \cdots] / [\sigma_{in} + \sigma_{n2n} + \sigma_{n3n} + \cdots]$. The multi-group average cross sections − the inelastic scattering cross section (σ_{in}), the (n,2n) cross section (σ_{n2n}), the (n,3n) cross section (σ_{n3n}), and the cross sections for other inelastic reactions − are evaluated in the incident energy group n. Therefore, a^{nN} is unity if the (n,2n), (n,3n), or other (n,xn) reactions are not present; otherwise, this quantity is greater than unity and must be accounted for in determining the exit weight of the neutron undergoing an inelastic scattering. For example, $a^{1N}\approx 2.0$ for ^{235}U and $a^{1N}\approx 1.1$ for ^{27}Al, where group 1 extends from 16.5 MeV to 21.2 MeV.

Consider an incident neutron that has been identified as undergoing a scattering reaction, and not a capture or fission reaction. The incident neutron energy E_0 measured in the LAB system is known, and corresponding multi-group n has been identified (See Section 3). The total microscopic scattering cross section $\sigma_{Ts}(E_0)$ for the scattering nuclide is given by the summation of the elastic scattering cross section $\sigma_s(E_0)$ and the inelastic scattering cross section $\sigma_{in}(E_0)$ plus other reactions:

$$\sigma_{Ts}(E_0) = \sigma_s(E_0) + \sigma_{in}(E_0) + \sigma_{n2n}(E_0) + \sigma_{n3n}(E_0) + \cdots$$

Knowing the scattering nuclide, a random number (ξ) is used to decide whether the scattering is inelastic or elastic. All random numbers ξ or ξ_i used in this paper are pseudorandom numbers on the interval [0,1), i.e., $0\leq\xi<1$, and obtained from a pseudorandom number generator. The random number index i is introduced to indicate that random number ξ_i is unique and different from the previous random number ξ_{i-1}. If $\xi > [\sigma_s(E_0) / \sigma_{Ts}(E_0)]$, then the scattering is inelastic; otherwise, it is elastic.

3. ENERGY OF EMERGING NEUTRONS IN THE LAB SYSTEM

The spatial coordinates of a collision point and corresponding material composition at the collision point are determined through geometry tracking. The spatial coordinates, together with the energy (E_0), and direction cosines of the incident neutron, constitute a description of the incident neutron. After the collision the exit neutron values for the LAB energy and direction cosines are determined (per Section 5), and then the free-flight to the next collision point is determined. All exit parameters from the current collision become the incident parameters for the next collision.

The initial multi-group containing the incident energy is determined first. The incident neutron energy E_0 measured in the LAB system is known and is in multi-group n, i.e., $E_{n+1} \le E_0 < E_n$. This is done by starting with the lower cut-point of the first multi-group (E_n with n=2), and checking through subsequent lower cut-points, until inequality $E_{n+1} \le E_0$ is satisfied.

Following inelastic scattering, the exit-energy group is determined using the energy transfer matrices. First, define $RANN = \xi_1 \cdot a^{nN}$, where ξ_1 is a new random number. Then determine multi-group m containing the exit energy by checking until the inequality $RANN < a^{nm}$ is satisfied starting with m=n. Note that $m \ge n$ is always required. If the exit group is different from the initial group, then the exit energy is uniformly sampled within that group. If the exit group and the initial group are the same, then the LAB exit energy is uniformly sampled over the energy range extending from the incident energy to the lowest energy of the initial group. That is, when within-group inelastic scattering occurs, the exit energy is not allowed to be larger than the incident energy. The LAB exit energy E' is sampled by the following linear interpolation algorithm:

E_m and E_{m+1} are the upper and lower cut-points of multi-group m.
If $m>n$, set $ETOP = E_m$. Otherwise (i.e., m=n), set $ETOP = E_0$.
If $m \ge 2$, set $ANM1 = a^{n,m-1}$. Otherwise (i.e., m=1), set $ANM1 = 0$.

$$E' = E_{m+1} + (ETOP - E_{m+1}) \frac{a^{nm} - RANN}{a^{nm} - ANM1}.$$

4. SCATTERING ANGLE OF EMERGING NEUTRONS IN THE LAB SYSTEM

The energy and scattering angle of a neutron emerging from inelastic scattering are sampled independently since its initial kinetic energy is not conserved. When inelastic scattering is assumed isotropic in the CM system, the cosine of the scattering angle in the CM system (μ_c) is sampled uniformly by $\mu_c = 2\xi_2 - 1$. When the inelastic scattering is anisotropic, then angular distribution functions can be used to determine an appropriate μ_c value. A classic two-body collision kinematics problem is analyzed in this section to formulate the LAB scattering angle in terms of μ_c and the exit energy in the CM system as well as in the LAB system.

4.1 Two-Body Collision Kinematics in Two Coordinate Systems

In the energy region of interest, i.e., the region below ~20 MeV, inelastic scattering takes place primarily through the formation and decay of a compound nucleus. The interaction is analyzed by considering only the kinematics of the incoming and outgoing particles and ignoring completely the existence of the compound nucleus as an intermediate state. Also assumed is that the compound nucleus formed by an incoming neutron will emit only one neutron. Calculations of the kinematics of neutron interactions are considerably simplified when the interactions are described in the CM system [6]. The target nucleus is assumed to be at rest in the LAB system. Defined are

A = the atomic mass of the target nucleus in units of the neutron mass,
V = the speed of the center-of-mass of the two interacting particles as observed in the laboratory reference frame,
v_c = the speed of the neutron in the CM system before collision,
v_c' = the speed of the neutron in the CM system after collision,
v_L = the speed of the neutron in the LAB system before collision, and
v_L' = the speed of the neutron in the LAB system after collision.

By definition, when the target is at rest before the collision, the center-of-mass speed is

$$V = \frac{v_L}{A+1}. \quad (1)$$

Expressing the neutron speed $v=\sqrt{2E/m}$ in terms of its kinetic energy E and mass m, Eq. (1) yields

$$\begin{aligned}\frac{V}{v'_c} &= \frac{v_L}{v'_c\ (A+1)} \\ &= \frac{\sqrt{E_0/E'_c}}{A+1},\end{aligned} \tag{2}$$

where E'_c is the neutron exit energy measured in the CM system.

In either elastic or inelastic scattering, neutrons emerge at some angle with respect to their incident direction. The total momentum of the neutron and the target nucleus in the CM system is precisely zero before and after the collision. Consequently, if only two particles emerge from a collision, they must travel in opposite directions when observed in the CM system. Consider the scattering of a neutron as seen below in the LAB system and in the CM system. Viewed in the LAB system, the incident neutron moves with speed v_L and strikes the nucleus which is initially at rest. As a result of the collision, the neutron emerges with speed v'_L at angle θ_L with respect to its original direction, and the nucleus recoils in another direction. Viewed from the CM system, the neutron (with speed v_c) and the nucleus are observed to approach each other before collision. After the collision, the scattered neutron (with speed v'_c) and nucleus leave in opposite directions with the neutron scattering angle θ_c measured with respect to the incident direction.

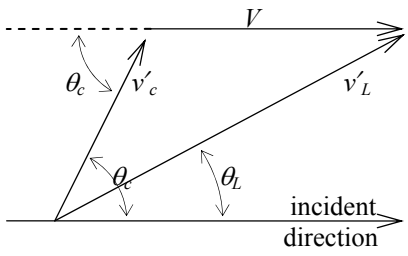

The incident-direction components of the velocity vector of the scattered neutron viewed in the two coordinate systems are therefore related by

$$v'_L\ \cos\theta_L = v'_c\ \cos\theta_c + V. \tag{3}$$

Defining the cosine of the CM scattering angle $\mu_c \equiv \cos\theta_c$ and the cosine of the LAB scattering angle $\mu_L \equiv \cos\theta_L$, we can show

$$\mu_L = \left(\frac{V}{v'_c} + \mu_c\right)\frac{v'_c}{v'_L}. \tag{4}$$

Depending on how the speed terms in Eq. (4) are transformed to other quantities, μ_L can be formulated in terms of either the CM exit energy or the LAB exit energy, as presented below.

4.2 LAB Scattering Angle in Terms of CM Exit Energy

To determine the ratio of the exit neutron speed in the CM system to that in the LAB system (v'_c/v'_L) that appears in Eq. (4), we apply the law of cosines to the triangle formed by the three velocity vectors (of magnitudes v'_L, v'_c, and V shown in the diagram above) to obtain

$$v'^{\,2}_L = v'^{\,2}_c + V^2 + 2v'_c V\ \mu_c\ , \tag{5}$$

and consequently

$$\left(v'_L/v'_c\right)^2 = \left(V/v'_c\right)^2 + 2\left(V/v'_c\right)\mu_c + 1. \tag{6}$$

Substituting Eq. (6) into Eq. (4), we obtain

$$\mu_L = \frac{(V/v_c') + \mu_c}{\sqrt{(V/v_c')^2 + 2(V/v_c')\mu_c + 1}}. \quad (7)$$

Defining "the CM-energy-mass factor" $\gamma_c \equiv \sqrt{E_0/E_c'}\,/(A+1)$ and using Eq. (2), we can rewrite Eq. (7) as follows:

$$\mu_L = \frac{\gamma_c + \mu_c}{\sqrt{(\gamma_c + \mu_c)^2 + 1 - \mu_c^2}}. \quad (8)$$

Equation (8) is analogous, but identical in principle, to one of the scattering formulas presented in Reference 6 for an inelastic reaction that was prescribed in an excitation-energy level method. Using Eqs. (2) and (4) and a neutron speed-energy equivalency $v_c'/v_L' = \sqrt{E_c'/E'}$, we can show when μ_c is very close to zero that $\mu_L \approx \gamma_L$, where $\gamma_L \equiv \sqrt{E_0/E'}\,/(A+1)$. We shall call γ_L "the LAB-energy-mass factor". Equation (8) can also be applied to *elastic* scattering with the target at rest where γ_c reduces to the well-known "inverse-mass factor" A^{-1}, the ratio of the mass of the neutron to that of the target. This is because the kinetic energy of the neutron in CM system is unaltered by the elastic scattering.

4.3 RCP01 Approximation of CM Exit Energy

When the inelastic multi-group energy transfer matrix for a target nuclide used in a Monte Carlo code is defined in terms of LAB neutron energies, the matrix does not provide E'_c values, and thus γ_c is not known. The RCP01 code uses an approximation to the CM-energy-mass factor γ_c in Eq. (8):

$$\gamma_c \leftarrow \frac{\sqrt{E_0/E'}}{A+1}, \quad (9)$$

where E' (the exit energy in the LAB system) has replaced E'_c in the definition of γ_c. The cosine of the LAB scattering angle defined in Eq. (8) and determined using the Eq. (9) approximation for γ_c will be called $\tilde{\mu}_L$. This approximation is accurate for very heavy targets (A>>1) and for certain values of μ_c, as demonstrated in Figure 1. Otherwise, the approximation is inadequate. Certain Monte Carlo codes that use multi-group energy transfer matrix methods use even simpler approximations: The MCU code assumes that the inelastic scattering is isotropic in the LAB system (i.e., $\mu_L = 2\xi - 1$). MCU was developed at Kurchatov Institute in Russia for reactor design applications and uses a group transfer matrix approach like the one employed in RCP01 and RACER. In its multi-group mode calculations, the VIM code [4] approximates within-group inelastic scattering as elastic scattering in which no energy is lost, and assumes out-of-group inelastic scattering to be isotropic in the LAB system.

Inserting Eq. (2) into Eq. (6) and using the definition of γ_c, we can obtain a useful formula that can transform the exit neutron energy determined in the CM system (E'_c) to the corresponding exit energy in the LAB system (E'):

$$E' = E_c'\,(\gamma_c^{\,2} + 2\,\mu_c\,\gamma_c + 1). \quad (10)$$

Using the relationship $\sqrt{E_c'/E'} = \gamma_L/\gamma_c$, Eq. (10) yields a relationship between the two energy-mass factors γ_c and γ_L:

$$\frac{\gamma_L}{\gamma_c} = \frac{1}{\sqrt{\gamma_c^{\,2} + 2\mu_c\gamma_c + 1}}. \quad (11)$$

The ratio γ_L/γ_c is close to unity for any μ_c value when γ_c approaches zero (e.g., for inelastic scattering with an infinitely heavy target or for a small change in neutron energy) or for certain negative μ_c values that meet a condition $\mu_c = -0.5\,\gamma_c$. For positive μ_c values, γ_L is always smaller than γ_c. Characteristics of the γ_L/γ_c ratio are depicted in

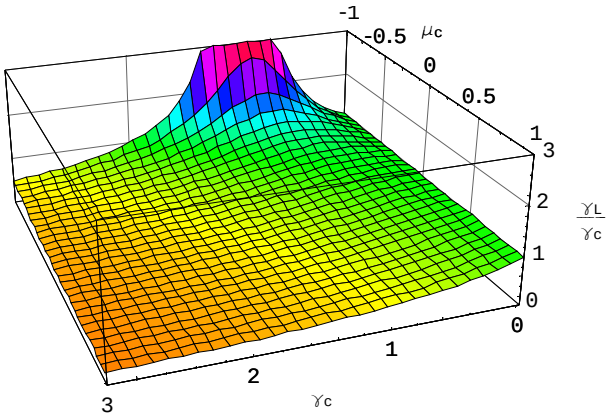

(a) Ratio γ_L/γ_c , Eq. (11)

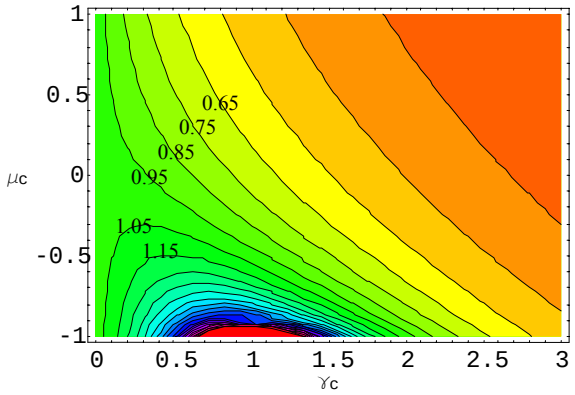

(b) Contour Plot of γ_L/γ_c

Figure 1
Comparison of the LAB and CM Energy-Mass Factors γ_L and γ_c

Table I. Error in LAB Scattering Angles Due to CM Exit Energy Approximated by LAB Exit Energy

Selected Input		γ_L from Eq. (11)	LAB Scattering Angle (degrees)		Error in LAB Scattering Angle	
μ_c	γ_c		True ($\cos^{-1}\mu_L$)	Approximate * ($\cos^{-1}\tilde{\mu}_L$)	degrees	percent
0.6	0.9	0.5294	28.1	35.3	7.2	25.6
0.6	0.7	0.4586	31.6	37.1	5.5	17.4
0.6	0.5	0.3676	36.0	39.6	3.6	10.0
0.3	0.7	0.5065	43.6	49.8	6.2	14.2
0.6	0.1	0.0941	48.8	49.1	0.3	0.6
0.3	0.5	0.4016	50.0	53.7	3.7	7.4
0.0	0.7	0.5735	55.0	60.2	5.2	9.5
0.0	0.5	0.4472	63.4	65.9	2.5	3.9
−0.6	1.0	1.1180	63.4	57.1	−6.3	−9.9
−0.3	0.7	0.6767	67.3	68.5	1.2	1.8
−0.6	0.9	1.0533	69.4	60.5	−8.9	−12.8
0.0	0.3	0.2873	73.3	74.0	0.7	1.0
−0.3	0.5	0.5130	78.2	77.4	−0.8	−1.0
−0.6	0.7	0.8682	82.9	71.5	−11.4	−13.8
0.0	0.01	0.0100	89.4	89.4	0.0	0.0
−0.6	0.5	0.6202	97.1	88.6	−8.5	−8.8
−0.6	0.1	0.1060	122.0	121.7	−0.3	−0.2
−0.8	0.1	0.1085	139.4	139.1	−0.3	−0.2
−0.9	0.2	0.2425	148.1	146.5	−1.6	−1.1
−0.95	0.2	0.2462	157.4	156.1	−1.3	−0.8

* $\tilde{\mu}_L$ from Eq. (8) with γ_c replaced with γ_L determined by Eq. (11) using the given data μ_c and γ_c.

Figure 1 as a function of μ_c and γ_c. The contour plot (b) in Figure 1 shows a sequence of 27 equally-spaced contours (i.e., space=0.1) of γ_L/γ_c values ranging from 0.25 to 2.95 shown in the three-dimensional plot (a), with the left-most "*T*-shaped" green region that includes the $\gamma_c \approx 0$ realm being $0.95 < \gamma_L / \gamma_c < 1.05$.

An evaluation of the LAB scattering angles determined by Eqs. (8) and (11) for selected μ_c and γ_c data is presented in Table I. The evaluation data are presented in ascending order of the true LAB scattering angle given in the fourth column. For a given set of arbitrary μ_c and γ_c data, a corresponding γ_L value is determined by Eq. (11). The γ_c value was used in Eq. (8) to determine a "true" μ_L value, while the γ_L value was used in Eq. (8) to determine an "approximate" cosine value $\tilde{\mu}_L$. When $\mu_c \approx \pm 0.6$, the error in the approximate scattering angle ($\cos^{-1} \tilde{\mu}_L$) exceeds 10% for certain scattering conditions set by γ_L (i.e., depending on the target mass and the neutron energy transfer).

Since Eq. (11) is a second order equation in γ_c, one can solve the equation for γ_c in terms of γ_L and μ_c, first determine $\gamma_c + \mu_c$, and then determine μ_L using Eq. (8). However, the resulting γ_c formula can cause numerical difficulties if γ_L is very close to unity. Therefore, a direct μ_L solution that is computationally more efficient is developed by deriving a relationship between γ_c and γ_L.

4.4 LAB Scattering Angle in Terms of LAB Exit Energy

When Eq. (2) is inserted into Eq. (4), we have

$$\mu_c v_c' = \mu_L v_L' - \frac{v_L}{A+1}, \tag{12}$$

which is transformed to, when each term is divided by $v_L / (A+1)$,

$$\mu_c (A+1) \frac{v_c'}{v_L} = \mu_L (A+1) \frac{v_L'}{v_L} - 1. \tag{13}$$

Since the neutron speed v equals to $\sqrt{2E/m}$ for its kinetic energy E and mass m, Eq. (13) yields a relationship between γ_c and γ_L:

$$\frac{\mu_c}{\gamma_c} = \frac{\mu_L}{\gamma_L} - 1, \tag{14.a}$$

or

$$\gamma_c + \mu_c = \frac{\mu_c \mu_L}{\mu_L - \gamma_L}. \tag{14.b}$$

Inserting Eq. (14.b) into Eq. (8) produces the following quadratic equation for μ_L:

$$\mu_L^{\,2} - 2\gamma_L (1 - \mu_c^{\,2}) \mu_L + \gamma_L^{\,2} (1 - \mu_c^{\,2}) - \mu_c^{\,2} = 0. \tag{15}$$

Solving this equation for μ_L, we can obtain a new formula for the cosine of the LAB scattering angle μ_L:

$$\mu_L = \gamma_L (1 - \mu_c^{\,2}) \pm |\mu_c| \sqrt{1 - \gamma_L^{\,2} (1 - \mu_c^{\,2})}. \tag{16}$$

Figure 2 compares the true LAB scattering angle cosine (μ_L) computed by Eq. (16), shown in plot (a), with the approximation ($\tilde{\mu}_L$) made by Eqs. (8) and (9), shown in plot (b), which is the approximation used in RCP01. The cosine values are depicted as a function of γ_L and μ_c, where the range of γ_L is limited to 0~1. When γ_L approaches zero in Eq. (15), we see $\mu_L \approx \mu_c$ and $\tilde{\mu}_L \approx \mu_c$ in the plots, a case when the LAB scattering angle is accurately approximated by the CM scattering angle. This is an approximation that is used in the RACER Monte Carlo code [2] for any γ_L value.

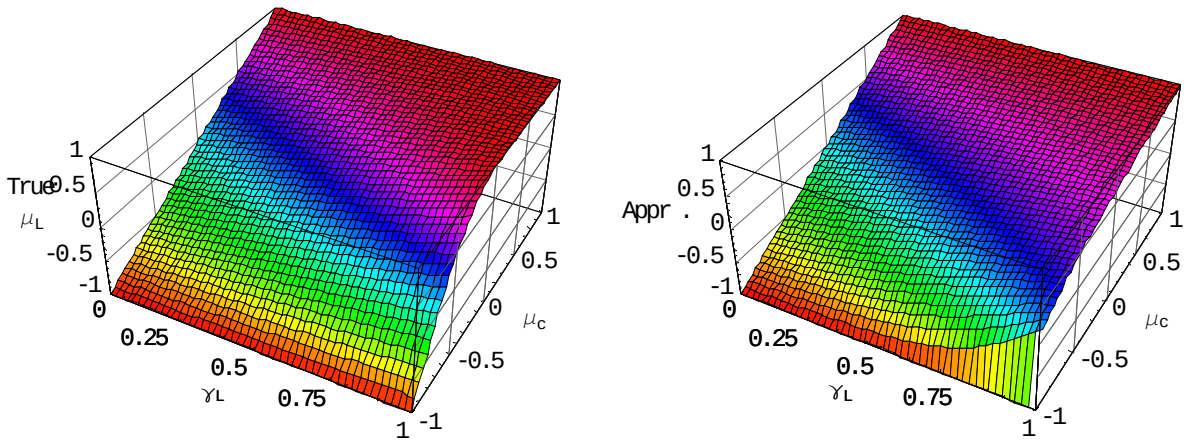

(a) True μ_L, as given by Eq. (16)

(b) Approximate $\tilde{\mu}_L$, Eq. (8) with γ_c Approximated by Eq. (9), i.e., $\gamma_c \leftarrow \gamma_L$

Figure 2
Comparison of True μ_L with Approximate $\tilde{\mu}_L$ as a Function of μ_c and γ_L

Figure 3 shows errors in $\tilde{\mu}_L$ in plot (a) as well as errors in $\cos^{-1}\tilde{\mu}_L$ in plot (b) that are incurred by the RCP01 approximation, relative to the true μ_L value formulated by Eq. (16). When the target nucleus is very heavy or the change in the neutron energy is very little and thus γ_L approaches zero, the approximation is adequate as discussed before. Figures 2 and 3 indicate that the RCP01 approximation is also adequate when the incident neutron scattering angle is small, i.e., $\mu_L \approx 1$ as well as $\tilde{\mu}_L \approx 1$ whenever $\mu_c \approx 1$. The approximation, however, can significantly mispredict certain exit neutron directions, especially at CM scattering angles ~80° ($\mu_c \approx 0.1$) and ~150° ($\mu_c \approx -0.9$), as shown in Figure 3-(c). The discrepancy between the true and approximate LAB scattering angles gradually increases as the μ_c value approaches zero (from the positive side), where the error in the approximate $\tilde{\mu}_L$ value becomes as large as ~30% (corresponding to an over-prediction by ~40° in the LAB scattering angle when $\mu_c \approx 0.1$ and $\gamma_L \approx 1$). When the μ_c value turns negative (i.e., backward scatterings in the CM system), the error in the approximate LAB scattering angle also becomes significant at certain values of γ_L, e.g., an under-prediction by ~60° when $\mu_c \approx 0.9$ and $\gamma_L \approx 1$.

The errors in the approximate LAB scattering angle determined in Table I for selected inelastic scattering conditions are identical to those shown in Figure 3-(c) for corresponding μ_c and γ_L values. Computing μ_L using Eq. (16) and its acceptance require certain conditions depending on the magnitude of γ_L and μ_c, as discussed in Section 4.5.

4.5 LAB-Energy-Mass Factor γ_L Exceeding Unity

Equation (16) is valid only for $[1-\gamma_L^2(1-\mu_c^2)] \geq 0$. Since the $(1-\mu_c^2)$ term can be as large as unity, the $[1-\gamma_L^2(1-\mu_c^2)]$ term can become negative when γ_L exceeds unity. The value of γ_L can exceed unity only when a neutron undergoing an inelastic scattering with a target of mass number A loses its kinetic energy by a factor of at least $(A+1)^2$, a condition which is rare. Inelastic scattering cannot occur unless the CM incident neutron energy is greater than the energy of the first excited state in the target nucleus. For an extreme case where the upper bound of the incident energy E_0 is ~20 MeV and the lower bound of the LAB exit energy E' is 5.53 keV, the mass number of the heaviest target nuclide that can result in $\gamma_L > 1$ is 59. Lighter targets could cause the negativity problem when γ_L exceeds unity, which could occur for inelastic scattering from energy levels that are comparable to the kinetic energy of the incident neutron. For heavier targets such as zirconium or uranium isotopes, however, the possibility of having $\gamma_L > 1$ is extremely low.

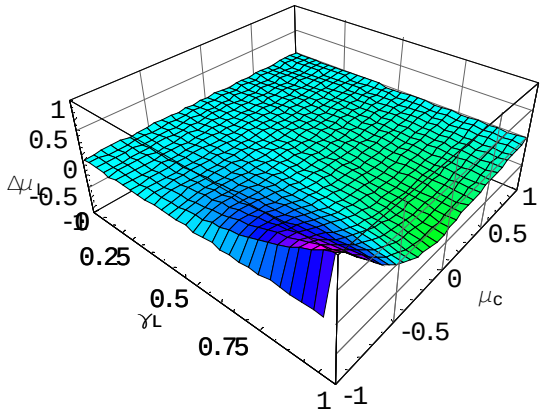

(a) Error in Approximate $\tilde{\mu}_L$, $\Delta\mu_L = \tilde{\mu}_L - \mu_L$

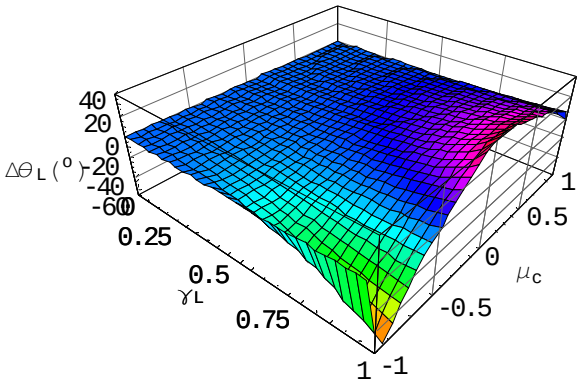

(b) Error in Approximate Angle ($\tilde{\theta}_L = \cos^{-1}\tilde{\mu}_L$), $\Delta\theta_L = \tilde{\theta}_L - \theta_L$ in degrees

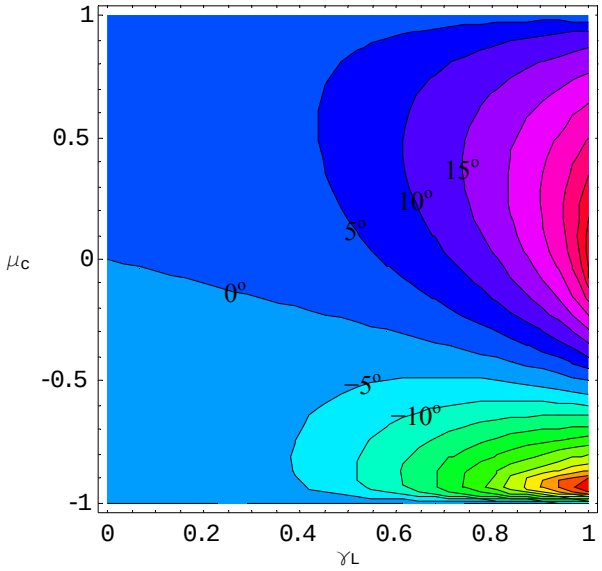

(c) Contour Plot of the Error in $\tilde{\theta}_L$, degrees

This contour plot shows a sequence of 22 equally-spaced contours (i.e., space=5°) of the error in the LAB scattering angle, $\tilde{\theta}_L = \cos^{-1}\tilde{\mu}_L$, approximated by Eq. (9) and ranging from −60° to 40°. The straight line that starts at $\mu_c = 0$ represents a linear relationship $\mu_c = -0.5\,\gamma_L$, where γ_L equals to γ_c, and, therefore, the approximation results in no error along the line. The regions above and below the straight line represent over-estimates and under-estimates of inelastic scattering angles, respectively.

Figure 3
Error in Approximate $\tilde{\mu}_L$ and in $\cos^{-1}\tilde{\mu}_L$ Due to Approximation of γ_c by Eq. (9), i.e., $\gamma_c \leftarrow \gamma_L$

When γ_L is greater than unity in Eq. (16), it places a limitation on the range of acceptable values of the cosine of the CM scattering angle μ_c:

$$\Gamma \le \mu_c \le 1 \text{ for positive } \mu_c \text{ values, where } \Gamma \equiv \sqrt{1-\gamma_L^{-2}}\ , \text{ and}$$
$$-1 \le \mu_c \le -\Gamma \text{ for negative } \mu_c \text{ values.}$$

That is, whenever $\gamma_L > 1$ and a μ_c value sampled falls in the range $(-\Gamma, \Gamma)$, the μ_c value must be rejected and a new μ_c value shall be sampled until a new value satisfies the acceptable range limitation.

Re-sampling of μ_c could be computationally intensive, especially when $\gamma_L >> 1$ and the range of valid μ_c is confined to a narrow band close to either +1 or −1. The band subtends μ_c either between −1 and $-\Gamma$ for $\mu_c < 0$ or between Γ and +1 for $\mu_c > 0$. To overcome this drawback, a procedure has been developed to transform the original μ_c value sampled from the (−1, 1) range into the narrow band close to either −1 or +1. Applying a linear transformation

scheme between ranges (−1, 0) and (−1, –Γ), or between ranges (0, +1) and (Γ, +1), we get the μ_c value re-cast into the narrow bands as follows:

$$\text{If } \mu_c<0, \text{ then } \mu_c \leftarrow \mu_c - (1+\mu_c)\,\Gamma, \text{ and}$$
$$\text{if } \mu_c\geq 0, \text{ then } \mu_c \leftarrow \mu_c + (1-\mu_c)\,\Gamma.$$

This transformation scheme will cause exit neutrons to be biased somewhat toward the incident direction (μ_c=1, i.e., directly forward) and the opposite direction (μ_c = –1, i.e., directly backward) when observed in the CM system. One of the conditions, $\Gamma \leq \mu_c \leq 1$ imposed here for positive μ_c values, however, will no longer be necessary because μ_c must not be positive whenever γ_L exceeds unity as discussed further in Section 4.6.

As discussed before, the condition of having γ_L>1 is extremely rare even with light targets. For example, when an incident neutron of 11 MeV kinetic energy undergoes an inelastic scattering with a boron isotope (^{11}B nucleus), the probability of seeing an emerging neutron of ~24 keV kinetic energy or smaller that results in γ_L>1.77 is only ~0.001. For the same incident condition, the probability of having γ_L > 0.81 (corresponding to exit energy ~116 keV) is ~0.01. Therefore, the conditions discussed here for γ_L>1 may be ignored, and the inelastic scattering that results in γ_L>1 may be completely ignored and a new collision process can start.

4.6 Dual Quantity of μ_L Value

The dual nature of μ_L due to the presence of the $\pm|\mu_c|$ term in Eq. (16) requires special attention. Equation (14.a) implies an important condition on μ_c and μ_L since both γ_c and γ_L are positive, namely

$$\frac{\mu_c}{\mu_L - \gamma_L} > 0. \tag{17}$$

This condition implies that (i) when μ_c is positive, $[\mu_L - \gamma_L]$ must be positive, and (ii) when μ_c is negative, $[\mu_L - \gamma_L]$ must be negative. One particular case of condition (ii) is that when γ_L is greater than unity, the $[\mu_L - \gamma_L]$ term becomes negative, and thence μ_c needs to be negative. Therefore, whenever γ_L exceeds unity, any positive μ_c must be discarded and a negative μ_c should be sampled. An alternative is to discard both the exit energy in the LAB system (E') and the positive μ_c, and then sample a new set of E' and μ_c until they together satisfy all conditions. Consequently, one of the conditions, $\Gamma \leq \mu_c \leq 1$ imposed earlier in Section 4.5 for positive μ_c values when γ_L>1, is no longer necessary.

The transformation of Eq. (14.a) to Eq. (14.b) was preconditioned by necessary conditions $\mu_c \neq 0$ and $\mu_L - \gamma_L \neq 0$, and, therefore, Eq. (16) is subject to the same conditions. When $\gamma_L = 1$, Eq. (16) yields $\mu_L = 1 - \mu_c^2 \pm \mu_c^2$, that is, either $\mu_L = 1$ or $\mu_L = 1 - 2\mu_c^2$. Since $\mu_L = \gamma_L$ is valid only when $\mu_c = 0$ and since $\mu_L \neq \gamma_L$ is required for arbitrary non-zero μ_c values, a general solution of μ_L for $\gamma_L = 1$ should be $\mu_L = 1 - 2\mu_c^2$, and not $\mu_L = 1$. This requires the $\pm|\mu_c|$ term be reduced to $+\mu_c$. This requirement results in a modification of Eq. (16) as follows:

$$\mu_L = \gamma_L(1-\mu_c^2) + \mu_c\sqrt{1-\gamma_L^2(1-\mu_c^2)}\,. \tag{18}$$

When μ_c is very close to zero (e.g., $-10^{-3} < \mu_c < 10^{-3}$), Eq. (14.a) is used to set $\mu_L = \gamma_L$. It is not difficult to demonstrate that Eq. (18) meets the two conditions (i) and (ii) implied above by Eq. (17) for positive and negative μ_c values, respectively. The conditions and procedures pertaining to the application of Eq. (18) are illustrated in Figure 4.

To complete the collision process, we need to determine direction cosines of the velocity vector of the neutron emerging from inelastic scattering. Since the direction cosines are not the subject of this paper, they are presented below for information only.

5. DIRECTION COSINES OF EXIT NEUTRON VELOCITY VECTOR

Incident direction cosines Ω_x, Ω_y, and Ω_z are defined as the cosine of the angle between the incident neutron velocity vector and the Cartesian *x, y*, and *z* axes, respectively, of a reference frame where the collision site is located

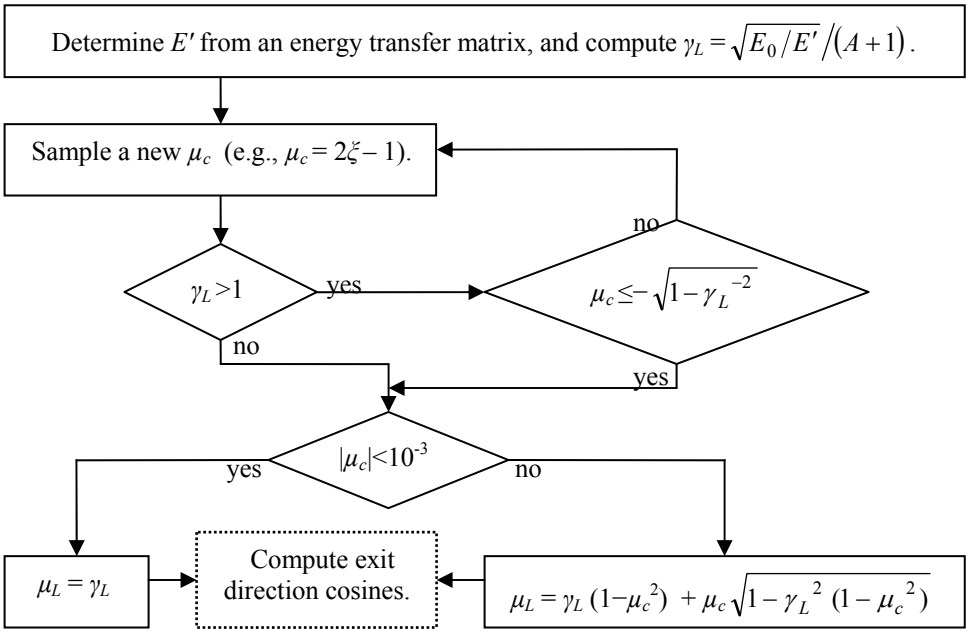

Figure 4
Sampling of LAB Scattering Angle Cosine μ_L

at the origin of the coordinate frame. The azimuthal angle φ is assumed isotropic. This assumption is justified because most scattering media of interest are isotropic in composition, and hence there is no preference toward any particular value of φ. The azimuthal angle is sampled uniformly in the range of [0, 2π) by $\varphi = 2\pi\,\xi_3$.

The exit direction cosines Ω'_x, Ω'_y, and Ω'_z of the neutron velocity vector relative to the Cartesian *x, y*, and *z* axes, respectively, are determined in terms of μ_L, φ, and incident direction cosines Ω_x, Ω_y, and Ω_z as follows:

$$\Omega'_x = \mu_L\,\Omega_x - C_L\,C_x\cos\varphi,$$

$$\Omega'_y = \mu_L\,\Omega_y + (C_L/C_x)(\Omega_x\,\Omega_y\cos\varphi - \Omega_z\sin\varphi), \textit{ and}$$

$$\Omega'_z = \mu_L\,\Omega_z + (C_L/C_x)(\Omega_x\,\Omega_z\cos\varphi + \Omega_y\sin\varphi),$$

where $C_L \equiv \sqrt{|1-\mu_L^2|}$ and $C_x \equiv \sqrt{|1-\Omega_x^2|}$. The absolute value under the square root of C_L and C_x is introduced to avoid possible round-off errors when μ_L or Ω_x is close to unity or slightly exceeds unity even though such occasions would be extremely rare. Constant C_L should be set to zero whenever the value of $[1-\mu_L^2]$ becomes negative. For values of $|\Omega_x|$ very close to unity (e.g., $|1-\Omega_x^2| < 10^{-3}$), alternative formulae should be used to avoid machine round-off errors.

6. SUMMARY AND CONCLUSIONS

An algorithm is developed which accurately determines scattering angles of neutrons emerging from inelastic collisions of fast neutrons when the inelastic scattering is treated in a multi-group energy transfer matrix method. The development was designed to improve an existing approximation used in the RCP01 code. The new algorithm is based on a classic two-body collision kinematics problem. It has been developed with no approximations, and is accurate and easy to implement. A multi-group energy transfer matrix method used in the RCP01 code has been outlined. The accuracy improvement of the new algorithm is noticeable in inelastic scattering with light targets es-

pecially when neutrons lose a large portion of their incident energy. The current RCP01 approximation is adequate for relatively heavy target nuclides, however, the approximation can significantly mispredict certain exit neutron directions.

7. ACKNOWLEDGMENTS

The author would like to thank the following people for their help in both providing the incentive for and reviewing this work. Dr. J. P. Colletti (Bechtel Bettis, Inc), Dr. D. E. Dei (Naval Reactors, U. S. Department of Energy), Dr. A. C. Kahler (Bechtel Bettis, Inc.), and Dr. T. M. Sutton (KAPL, Inc.).

8. REFERENCES

1. L. A. Ondis II, L. J. Tyburski, and B. S. Moskowitz, "RCP01 – A Monte Carlo Program for Solving Neutron and Photon Transport Problems in Three Dimensional Geometry with Detailed Energy Description and Depletion Capability," B-TM-1638, Bettis Atomic Power Laboratory (2000).

2. T. M. Sutton, et al., "The Physical Models and Statistical Procedures Used in the RACER Monte Carlo Code," KAPL-4840, U. S. Department of Energy – Office of Scientific and Technical Information (1999).

3. J. F. Briesmeister, "MCNP™ – A General Monte Carlo N-Particle Transport Code," LA-13079-M, Los Alamos National Laboratory (2000).

4. R. N. Blomquist, "VIM Monte Carlo Neutron/Photon Transport Code: User's Guide, Version 4.0," http://web.ra.anl.gov/vimguide/ (2000).

5. Cross Section Evaluation Working Group, "ENDF-102: Data Formats and Procedures for the Evaluated Nuclear Data File ENDF-6," BNL-NCS-44945, National Nuclear Data Center, Brookhaven National Laboratory (1997).

6. C. J. Everett and E. D. Cashwell, "Scattering Formulas for the Two-Particle Reaction," LA-5196-MS, Los Alamos Scientific Laboratory (1973).